Pis'ma v ZhETF, vol. 76, iss. 11, pp. 771 – 773

Confining string formed by P-vortices in the indirect $Z(2)$ projection of $SU(2)$ lattice gauge theory

V. G. Bornyakov[+*□1)], *A. V. Kovalenko*[*1)], *M. I. Polikarpov*[*1)], *D. A. Sigaev*[*1)]

[+] *Institute for Theoretical Physics, Kanazawa University, 920-1192 Kanazawa, Japan*

[*] *Institute for Theoretical and Experimental Physics, 117259, Moscow, Russia*

[□] *Institute for High Energy Physics RAS, 142280 Protvino, Russia*

Submitted 24 October 2002

We study the distribution of P-vortices near the confining string in the indirect $Z(2)$ projection of $SU(2)$ lattice gauge theory. We find that the density of vortices approaches the vacuum value at large distances and is strongly suppressed near the line connecting the test quark–antiquark pair. This implies that the condensate of P-vortices is broken inside the confining string. The width of the P-vortex density distribution increases with increasing distance between the quark and antiquark. Our best fit indicates the logarithmic dependence of this width on $q\bar{q}$ separation distance.

PACS: 11.15.Ha, 11.25.Sq

1.Introduction. It was suggested by 't Hooft and Mandelstam that the string formation between the massive quark and antiquark was an analogue of the dual Meissner effect in a superconducting vacuum [1], and the most popular theory of the quark confinement was based on the abelian projection [2].

There are also alternative theories of the quark confinement. It was found recently that one of them, the magnetic vortex theory [3], did not have some drawbacks of the abelian projected theory. The most remarkable success of the magnetic vortex theory is an explanation of the existence of the linear potential between higher representation quarks in the Casimir scaling regime [4].

While in the abelian projected theory, the part of the $SU(N)$ symmetry is broken leaving $U(1)^{N-1}$ gauge symmetry, in the magnetic vortex theory, the Z_N center plays a special role. Thus, further gauge fixing, which leaves a remnant $Z(N)$ symmetry, is to be performed.

This may be achieved in several ways. First, we can directly fix the gauge in $SU(N)$ theory leaving $Z(N)$ gauge symmetry [4]. We can also use the indirect $Z(2)$ projection [4]. It is defined in terms of abelian variables, i. e. we have to perform the abelian projection first. After fixing the maximal abelian gauge [5] and projecting $SU(2)$ link variables $U_{x\mu}$ onto abelian link variables $u_{x\mu}$ we maximize the functional R and define the link variables $Z_{x\mu}$:

$$R = \sum_{x,\mu} \cos^2 \theta_{x\mu},$$

$$Z_{x\mu} = \mathrm{sign}(\cos\theta_{x\mu}),$$

where $\cos\theta_{x\mu} = \frac{1}{2}\mathrm{Tr}\, u_{x\mu}$.

A plaquette is pierced by a P-vortex lying on the dual lattice if $Z(2)$ plaquette $P_{x,\mu\nu} \equiv Z_{x\mu} Z_{x+\mu,\nu} Z^{\dagger}_{x+\nu,\mu} Z^{\dagger}_{x\nu} = -1$.

Below we present the results of the study of the confining string in terms of P-vortices. Having applied the indirect $Z(2)$ projection to the original $SU(2)$ configurations for various lattice sizes and couplings β, we obtained reliable results for the form of $Z(2)$ confining string and the dependence of its radius on the distance between the test quark and antiquark.

2. Vortices near the confining string. We consider the quantity that measures the dependence of the vortex density on the distances $r_\perp$ from the $q\bar{q}$ axis and $r_\parallel$ along this axis

$$Q(r_\perp, r_\parallel) = \frac{<WV(r_\perp, r_\parallel)>}{<W>}, \qquad (1)$$

where W is a $Z(2)$ Wilson loop and vortex detector $V(r_\perp, r_\parallel) = (1 - P_{x,\mu\nu})/2$. The similar quantity was investigated for the distribution of monopole currents near the confining string [6]. Our calculations were performed on $Z(2)$ vacuum configurations obtained via the indirect $Z(2)$ projection, the intermediate gauge fixing being performed by the simulated annealing algorithm [7]. Table summarizes the information about configurations used.

Since a P-vortex is a 2-dimensional surface in the 4-dimensional space, the P-vortex density is defined on the plaquettes and has 6 independent components for each site. Thus the complete measurement of the P-vortex density involves measurements of 6 quantities per

[1)] e-mail: vborn@itep.ru; kovalenko@itep.ru; polykarp@itep.ru; sigaev@itep.ru

site, or one quantity per plaquette. We use the notation '01', '02' etc. to denote the orientation of the vortex detector $V(r_\perp, r_\|)$, where '0' denotes the temporal direction of the $Z(2)$ Wilson loop, '1' denotes the spatial direction of the $Z(2)$ Wilson loop, and '2' is the direction in which $r_\perp$ is counted, so that the densities for planes 'μ 2' and 'μ 3' may differ (and actually do so).

Obviously there is no correlation between W and $V(r_\perp, r_\|)$ at large distances $r_\perp$, $Q(\infty, r_\|) = <V>$, which is the value of the vacuum vortex density [8]. However, the vortex density decreases near the confining string. This effect is illustrated in Fig.1. The minima on Fig.1 correspond to the positions of the test quark

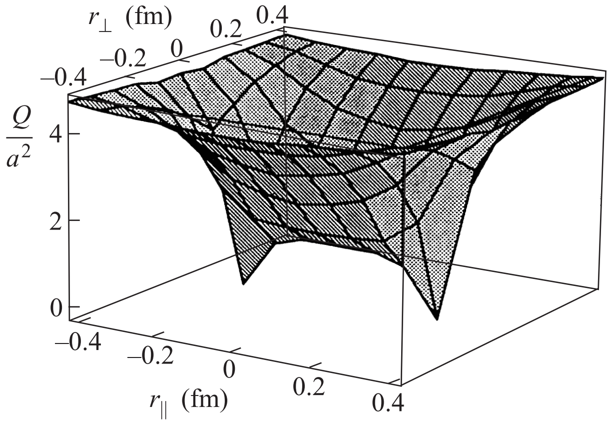

Fig.1. The dependence of Q/a^2 on $r_\perp$ and $r_\|$, $\beta = 2.5$

and antiquark. This figure actually represents only one of the six components of vortex density, '01', but the others look rather similar.

In Fig.2 we show the dependence of all six components of the vortex density $Q(r_\perp, r_\|)/a^2$ on the distance $r_\perp$ for $r_\|$ fixed in the middle of the $q\bar{q}$ axis and the vortex detector V lying in various planes. We see stronger suppression of Q for the plane '01' which is parallel to the Wilson loop. The normalization $1/a^2$ is due to dimensional reasons [4]; the density of P-vortices, which are 2-dimensional surfaces, should scale as a^2, a being the lattice spacing.

3. The radius of the confining string. We employ $Q(r_\perp, r_\|)$ to evaluate the radius of the confining string in terms of P-vortices.

Simulation details

β	lattice size	number of configurations
2.40	24^4	20
2.50	24^4	50
2.55	28^4	50
2.60	28^4	25

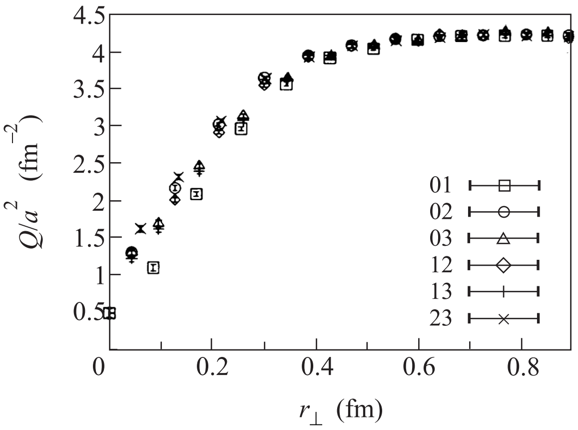

Fig.2. Q/a^2 as the function of $r_\perp$ for the Wilson loop 11×5, $\beta = 2.5$. Notation '01' means that the detecting plaquette lies in the plane '01'

The Gaussian form of the fitting function is used to fit our data:

$$Q(r_\perp) = A \exp\left[-\left(\frac{r_\perp}{r_0}\right)^2\right] + Q(\infty), \qquad (2)$$

A and r_0 being the fitting parameters. It is reasonable to treat r_0 as the radius of the confining string. Function (2) has been used in studies of the nonabelian [9] and abelian [10] flux tubes action density and has been predicted theoretically in [11]. We obtained fits with reasonable χ^2 (Fig.3).

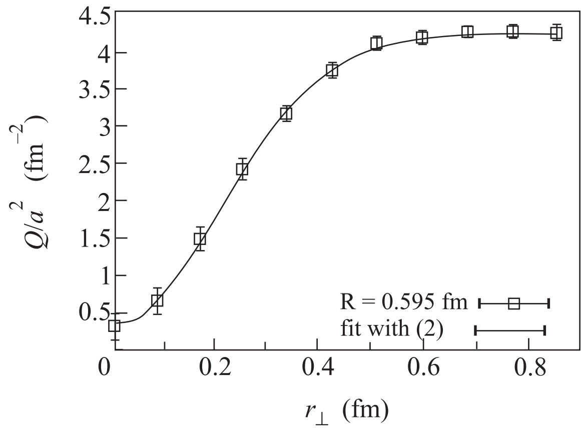

Fig.3. The fit of the confining string profile by expression (2) for the Wilson loop 11×9, $\beta = 2.5$. The data are for plaquettes '01'

To determine the dependence of the radius r_0 on the distance R between the quark and antiquark we involve the data for four different β and various sizes of Wilson loops. Different β yield results which are in a good agreement (Fig.4), thus confirming that our results correspond to the continuum limit.

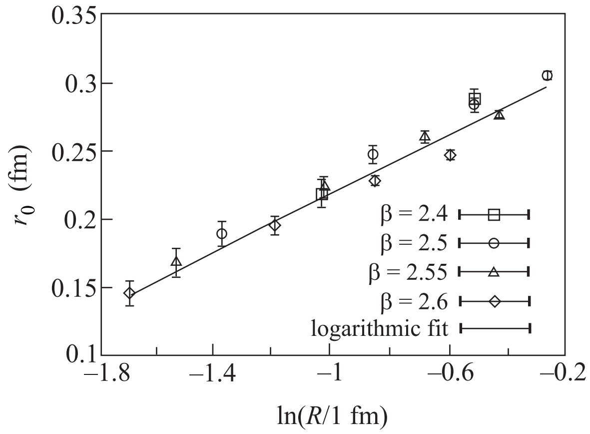

Fig.4. The confining string radius as a function of $\ln R$

We used several fitting functions to describe the dependence of r_0 on R; the best χ^2 was obtained for

$$r_0(R) = a \ln(R/1\,\mathrm{fm}) + b, \tag{3}$$

which is shown on Fig.4 by the solid line; $\chi^2/n_{\mathrm{free}} = 4.43$, $a = 0.107(8)$ fm, $b = 0.326(6)$ fm. A little bit worse fit ($\chi^2/n_{\mathrm{free}} = 4.47$) was obtained for the fitting function $r_0(R) = (aR + b)^\alpha$ with one extra free parameter α. The fit using the dependence $r_0(R) = (a \ln(R/1\,\mathrm{fm}) + b)^{1/2}$, which is predicted by the simple string model [11], gives a worse $\chi^2/n_{\mathrm{free}} = 5.89$.

It is worth mentioning that the logarithmic dependence of r_0^2 has been found out in the studies of the nonabelian flux tube [9], while for the abelian flux tube the width was found to be independent on R [10]. On the other hand, the accurate recent studies show the dependence of the width of the abelian flux tube on the distance between the test quark–antiquark pair (Y. Koma, private communication).

Note that on Fig.4 even data for very small $R \approx 0.2$ fm seem to lie on the same curve as data for larger R (till $R \approx 0.8$ fm). This means that the confining string is already formed at very small distances. This fact is in agreement with the results of Ref. [4], where the correct value of the string tension has been obtained from small $Z(2)$ Wilson loops.

4. Discussion. For the monopole confinement mechanism there exists the effective classical model, which is the dual abelian Higgs model. The classical equations of motion for this model describe unexpectedly well the profile of the confining string in the maximal abelian projection [6]. For P-vortices we have no classical effective model, and our fitting function (2) has a phenomenological origin. On the other hand, the qualitative similarity of the dependence of $Q(r_\perp, r_\parallel)$ on $r_\perp$ to the dependence of the action density of the nonabelian or abelian flux tube is not accidental. $Q(r_\perp, r_\parallel)$ can be interpreted as $Z(2)$ projection of the nonabelian magnetic/electric energy density. This aspect will be discussed elsewhere.

We can also explain the flux tube profile shown in Fig.1 from another point of view. It is well known that monopoles are correlated with P-vortices [4]. On the other hand, it is also known that the condensate of monopoles is broken inside the confining string. Thus one can expect that the condensate of P-vortices should be also broken or at least substantially reduced inside the confining string. We really see this effect in Figs.1–3.

The authors are grateful to M. N. Chernodub, F. V. Gubarev and V. I. Zakharov for useful discussions. M. I. P. is partially supported by grants RFBR # 02-02-17308, # 01-02-117456, # 00-15-96-786, INTAS-00-00111, and CRDF award # RPI-2364-MO-02. A. V. K. is partially supported by grants RFBR 02-02-17308 and CRDF MO-011-0. B. V. G. acknowledges support by JSPS Fellowship grant.

1. G. 't Hooft, *High Energy Physics*, Ed. A. Zichichi, Editrice Compositori, Bolognia, 1976; S. Mandelstam, Phys. Rept. **23**, 245 (1976).
2. G. 't Hooft, Nucl. Phys. **B190**, 455 (1981).
3. G. 't Hooft, Nucl. Phys. **B138**, 1 (1978); J. M. Cornwall, Nucl. Phys. **B157**, 392 (1979).
4. L. Del Debbio, M. Faber, J. Greensite, and S. Olejnik, Phys. Rev. **D55**, 2298 (1997) [arXiv:hep-lat/9610005]; M. Faber, J. Greensite, and S. Olejnik, Phys. Rev. **D57**, 2603 (1998) [arXiv:hep-lat/9710039].
5. A. S. Kronfeld, G. Schierholz, and U. J. Wiese, Nucl. Phys. **B293**, 461 (1987).
6. V. Singh, D. A. Browne, and R. W. Haymaker, Phys. Lett. **B306**, 115 (1993) [arXiv:hep-lat/9301004]; C. Schlichter, G. S. Bali, and K. Schilling, Nucl. Phys. Proc. Suppl. **63**, 519 (1998) [arXiv:hep-lat/9709114]; F. V. Gubarev, E. M. Ilgenfritz, M. I. Polikarpov, and T. Suzuki, Phys. Lett. **B468**, 134 (1999) [arXiv:hep-lat/9909099].
7. V. G. Bornyakov, D. A. Komarov, and M. I. Polikarpov, Phys. Lett. **B497**, 151 (2001) [arXiv:hep-lat/0009035].
8. M. N. Chernodub, M. I. Polikarpov, A. I. Veselov, and M. A. Zubkov, Nucl. Phys. Proc. Suppl. **73**, 575 (1999) [arXiv:hep-lat/9809158].
9. G. S. Bali, K. Schilling, and C. Schlichter, Phys. Rev. **D51**, 5165 (1995) [arXiv:hep-lat/9409005].
10. G. S. Bali, arXiv:hep-ph/9809351; V. Bornyakov, H. Ichie, S. Kitahara et al., Nucl. Phys. Proc. Suppl. **106**, 634 (2002) [arXiv:hep-lat/0111042].
11. M. Luscher, G. Munster, and P. Weisz, Nucl. Phys. **B180**, 1 (1981).